TRACING BIOGEOCHEMICAL CHANGES WITHIN INTENSE DEEP-WATER INTRUSIONS IN PUGET SOUND, WA.

E. Boss[1], M. J. Perry and M. C. Talbot

Running head: Tracing intrusions in Puget Sound

Emmanuel Boss and Mary Jane Perry

University of Maine

School of Marine Sciences

5741 Libby Hall

Emmanuel.boss@maine.edu

MaryKay C. Talbot

University of Washington

School of Oceanography

[1] Corresponding author

ABSTRACT

Bottom water intrusions are one of the major circulation features of Puget Sound, Washington. These intrusions supply oxygen and chlorophyll rich surface waters to the depth of Puget Sound providing a pathway for oceanic phytoplankton species into the Sound.

In this paper we analyze observation on the formation of a deep-water intrusion at Admiralty Inlet, and characterize it for its hydrographical and bio-chemical properties. Subsequent observations, performed a week later within Puget Sound, provide information on bio-chemical transformation within the intrusive water. Most of the Chlorophyll and cyanobacteria-like cells are observed to decrease significantly in the intrusion. Phytoplankton respiration, however, explains only 30% of the reduction in oxygen within the intrusion, suggesting that respiration of additional organic material takes place within the deep water.

Flow-cytometric analysis reveals three dominating groups of particles. One of these has optical characteristics similar to a coastal cyanobacteria and has a half-life in the dark of about 6 days. This characteristic makes it a good temporal tracer for the intruding waters.

The predictability the sub-tidal circulation features in Puget Sound exhibited here as well as in other studies, suggests that it may be possible to maximize the flux of anthropogenic contaminant out of Puget Sound by timing their release and by modifying their density.

INTRODUCTION

Nestled between the Olympic Mountains to the west and the Cascade Mountain range to the East, Puget Sound is a semi-enclosed glacial fjord where salt water from the Pacific Ocean is overlaid with fresh water draining from the surrounding watershed. Puget Sound is deep, with an average depth of 150m and a maximal depth of nearly 300m. Puget Sound is made up of a

series basins and sills (Fig. 1). Admiralty Inlet, a relatively shallow sill, separates the waters of the Strait of Juan de Fuca from the waters of Puget Sound proper.

Bottom water intrusions are one of the major circulation features of Puget Sound, Washington (Canon et al., 1990) and are a major source of sub-tidal variability (Bretschneider et al., 1985). Together with tidal pumping at the Narrows, intrusions are responsible for the short residence time of the deep water within the Main Basin of Puget Sound (about three weeks, Ebbesmeyer and Barnes, 1980) and are crucial to removal of anthropogenic contaminants and effluents from Puget Sound to the straits of Juan de Fuca and the Pacific Ocean. The short residence time is also reflected in the prevalence of oxygen rich conditions in Puget Sound, in contrast to other fjords whose deep waters are stagnant for long periods of time whose oxygen levels are low (e.g. Farmer and Freeland, 1983). Deep-water intrusions are formed during neap tides when the mixing over Admiralty Inlet sill is at a minimum (Cannon and Laird, 1978). Water intrusions formed during neap tides replaces the resident deep water within the Main Basin. When tidal mixing over the sills is more intense, intermediate water intrusions may occur with the formation of step-like density structure within the Main Basin.

The dynamics of chlorophyll-*a* concentration (chl *a*) at depth in Puget Sound have been linked to bottom water intrusions by Winter et al. (1975). In a time-series at a hydrographic station near the center of the Main Basin of Puget Sound they observed increased pigment concentrations associated with increased salinity and depth. They argued that sinking of cells could not account for their observations, but rather invoked advection. Here we support their argument by tracing a high chl *a* intrusion as it propagates from Admiralty Inlet into the bottom of the Main Basin of Puget Sound.

In the present paper we present observations from two hydrographic sections taken in April, 1997; the first section (C-I, Fig. 1) took place during an intense neap tide intrusion over the

Admiralty Inlet sill region and the second section (C-II, Fig. 1) was performed a week later within the Main Basin. We evaluate several biological and chemical characteristics of the intrusion for their potential to serve as tracers of the intrusion as well as the insight they provide into bio-chemical processes occurring within the intrusion.

METHODS

Hydrographic data were collected during two survey sections conducted aboard *Clifford A. Barnes* on April 13-14 (C-I) and 20(C-II) 1997. Hydrographic casts were performed at 18 stations (Fig. 1); additional casts were taken at Station (St.) 10, in mid basin, at the beginning and end of each of the two sections, to provide some guidance regarding temporal aliasing of the spatial transects. The first cruise was planned to coincide with the neap tide intrusion at Admiralty Inlet (Fig. 1), while the second one was intended to determine how far the deep-water intrusion propagated through the Main Basin during a one-week period. Additional hydrographic measurements were taken in between our two sections during a University of Washington student cruise to Whidbey Basin (St. 201, Fig. 1).

The sampling design (Fig. 1) followed the deepest route through the Main Basin and included bottom depressions where the densest water was expected to be found. The hydrographic sections were performed from north to south and occurred mostly during flood tides (Fig. 1). Station 10a was visited before section C-I was started to provide a reference for conditions prior to the intrusion. Station 10 was revisited at the end of C-I (as St. 10b) and at the beginning and end of C-II (as Sts. 10c and 10d).

Conductivity, temperature and pressure were measured with a SBE-11 CTD; a Sea-Tech transmissometer (25-cm path length) was used to measure light transmittance in the water. The CTD was lowered to within less than 10m off the bottom. Water samples were collected using 12

5-l Niskin bottles mounted on a rosette sampler. Triplicate discrete samples were analyzed for oxygen (Winkler titration), chl *a* and pheopigments concentrations (Holm-Hansen et al., 1965). In addition, samples for chl *a* and pheopigments concentrations associated with particles larger than 70 μm were also collected at discrete depths. Water was filtered through 70 μm -Nitex filters. The filters were analyzed for pigment concentrations and the filtrates were frozen in liquid nitrogen for flow cytometric analysis in the shore-based laboratory.

The hydrographic data (Fig. 2) were plotted using a weighted mapping technique (Roemmich, 1983). For the continuous-profile CTD data, a correlation function was chosen to be Gaussian with a horizontal correlation e-folding length of one station and a vertical correlation e-folding length of 5m. For the discrete samples, a variable vertical correlation was used that varied linearly from 10m near the surface to 80m at 250m. The average values of properties within the intrusion were calculated using the interpolated fields derived from the contouring method, with the constraint that the estimated relative error be smaller than 30%.

Flow-cytometric analyses were performed on an EPICS Profile flow cytometer. In general the low concentration of particles observed (i.e., a few hundred particles per ml) precluded statistical analysis of dynamics of changes in particle fluorescence characteristics within a group of particles (the error bars were larger than the changes in the signal). However, three different groups of particles were classified according to their fluorescence and scattering properties (Fig. 3). The classification was computed using a clustering analysis method; Red, orange fluorescence, and forward scatter data of each particle measured by the flow-cytometer were log transformed and calibrated relative to calibration beads. Clusters of particle were differentiated by their unique combination of red, orange fluorescence, and forward scatter. The differentiation was done by smoothing frequency data (20 point boxcar) and finding the minima between groups

of particles in regions where they were expected based on laboratory cultures. The same program was used to analyze all the data collected.

Two laboratory strains of *Synechococcus* were also analyzed by the flow cytometer, S. bacillaris (clone SYNG) and *Synechococcus* WH7803 (clone SYNDC2), respectively a coastal and a pelagic cyanobacterium (Olson et al., 1988). It was found that the distinct fluorescence and scattering patterns of groups F1 and F2 particle are similar as S. bacillaris and *Synechococcus* WH7803 respectively. Group F3 had fluorescence characteristics similar to F2 but with much greater forward scatter, presumably due to larger size. The identity of the F3 group is unknown, but these particles could potentially be fragments of fecal material or egested cells. This group is not analyzed further.

To assess the degree to which dilution from mixing of different water masses controlled the changes in particle concentration, 20 l water samples were taken from 10m at both St. 10b and St. 1 and from the bottom at St. 9. The water samples were stored at 8°C, in the dark, and were subsampled during the week between the cruises to provide a reference for changes observed in the intrusion waters during section C-II.

RESULTS

Hydrography

In the first section (C-I) a strong front is present between Sts. 5 and 6 (right panels, Fig. 2). This front is associated with intense downwelling that results from the interaction of the tidal flow and Admiralty Inlet's topography. Turner and Gregg (1995) observed and analyzed a similar feature at the same location.

Two intrusive water masses are observed during the C-I section: one to the north and one to the south of the front. The water mass to the south ($\sigma_\theta \sim 22.75$) has θ-S properties and high oxygen

and pigment concentrations indicative of a mixture of surface Puget Sound waters and oceanic waters. The temperature, pigment, and particularly the oxygen contours in Fig. 2 indicate that this water mass is intruding, at depth, into the Main Basin. We refer to this water mass as the 'early intrusion'.

To the north of the front, a tongue of dense ($23.2 > \sigma_\theta > 22.9$) water mass is present at the bottom extending from St. 1 to St. 6 and can be traced (along sloping isopycnals) to the surface in the Juan de-Fuca Straits (Fig 4). This water mass has similar hydrographic properties to those observed, a week later, at the bottom of the Main Basin. We refer to this dense water mass as the 'deep-water intrusion'.

Water properties in the bottom of Puget Sound at St. 10 (Fig. 5) indicate that by the end of the first section (10b) a warmer water mass is penetrating at depth, below 180m. A closer look reveals the existence of two maxima in temperature (one at 180m and a second next to the bottom). These data are suggestive of two separate intrusive features that can also be observed in the θ-S properties at St. 9 (Fig. 4). Each intrusive water mass is formed by a different mixture of oceanic and Puget Sound water, with the density determined by the proportion of each in the admixture.

Data from the C-II section, taken one week later, is shown in the left panels of Fig. 2. The waters below ~170m has the same θ-S properties as the dense deep-water intrusion in the C-I section. The conservation of θ-S properties in the intrusion indicates that this dense water penetrated with little mixing. These results are consistent with the notion that during neap tides mixing and modification of intruding oceanic waters are minimal.

The θ-S properties at depth at St. 201 in Whidbey Basin show a similar intrusive tongue as that observed at St. 9 during C-I (with, however influence of Puget Sound intermediate water, Fig. 4) implying that the early intrusion penetrates also into Whidbey basin. The θ-S properties at

the entrance of the Tacoma Narrows (St. 18) indicate that water there is upwelled from intermediate depths in the Main Basin (~100m, Fig. 2). Note that the water that resides at depth prior to the intrusion (bottom of St. 10a) was at about 70m during C-II (Figs. 4-5), uplifted by the deep intrusion and subsequent intermediate ones.

Biologically active tracers

A phytoplankton bloom ([chl *a*] > 8 mg m^{-3}) occurs at Sts. 5 and 6 during the C-I section. Downwelling of water with high chl *a* concentration is observed at 100m depth with subsequent entrainment into intermediate waters (Fig. 2). About 80% of the chl *a* concentration in the downwelling water is associated with the fraction of cells larger than 70μm (Fig. 2). This observation suggests that the bloom was due to large cells or chain-forming diatoms (diatom chains were present in a water sample collected from the surface at St. 1, S. Menden-Deuer, personal communication).

In the water comprising the deep-water intrusion only 40% of the chl *a* is associated with cells larger than 70 μm (Table 1), indicating that the oceanic waters in the Straits of Juan De Fuca contained relatively more small cells than the surface waters of Puget Sound. In contrast to the chl *a* distribution, a higher proportion of pheopigments (degradation products of chl *a* formed during zooplankton grazing of phytoplankton) are found in the size fraction smaller than 70 μm. At St. 10 prior to the intrusion, concentrations of chl *a* and pheopigments near the bottom are 0.24 and 0.4 mg m^{-3} respectively, much lower than concentrations within the deep intrusion (2.4 and 0.9 mg m^{-3} respectively, Table 1). A week later, chl *a* within the deep-water intrusion drops by more than 80% while pheopigments at depth has similar values to those in the intrusion tongue (~0.9mg m^{-3}).

Flow-cytometric analysis of the particles smaller than 70 μm (Fig. 6) revealed a single group that had significantly higher concentrations near the surface (F1, similar to the coastal cyanobacteria, SYNG, Fig. 3). This group also had a secondary concentration maximum associated with the intrusive waters at the bottom of the Main Basin during the second cruise. The distribution of the F1 particles near the Tacoma Narrows (Sts. 17 and 18) tracked the upwelling of intermediate waters into the Narrows and the mixing with waters with low concentrations of F1 particles. These data display clearly the effect of mixing at the Narrows in homogenizing water properties. Oxygen concentrations within the intrusion are reduced from 8.6 to 8.0ml l^{-1} during the week following the intrusion (Table 1, Fig. 2). Oxygen concentration decreases from North to South within the deep waters (Fig 2). Assuming a stochiometric ratio of 1.0 mol O_2 respired per 1.45 mol C oxidized and a gram ratio of C/chl *a* of 30, oxidation of the carbon associated with 2mg m^{-3} of chl *a* would result in the consumption of 0.2ml l^{-1}, about 30% of the observed reduction. Compared with the deep-water intrusion waters during C-I, concentration of F1 particles dropped from nearly 600 cells/200μl to 300 cells/200μl in the bottom of the Main Basin during C-II, due possibly to dilution, grazing and mortality. Prior to the intrusion there were nearly 90 cells/200μl of F1 at depth (St 10a). Group F2 had a small vertical gradient in comparison to F1 during C-II. Its values decrease from 200 cells/200μl near the surface to 130 cells/200μl near the bottom. Prior to the intrusion there were 70 F2 cells/200μl at the bottom of the Main Basin (St. 10a). In laboratory incubations of collected samples, the concentration of particles associated with phytoplankton (F1+ F2) was found to decrease by 40-60% after a week (data not shown). Assuming that the trophic dynamics within the incubation bottles were similar to those within the deep water, these observations suggest that little dilution occurred in the intrusive water body, as observed in the hydrography. Notice that the small cyanos are better preserved than other chl *a*

containing cells, as indicated by the reduction of the concentration of total and fractionated chl *a* by more than 80%.

DISCUSSION

The waters that penetrated with the deep water intrusion into the Main Basin of Puget Sound replaced the waters below 170m (Fig. 5). The volume of that water is approximately 7 km^3 (based on the 300m resolution, bathymetric data base compiled by Dr. Miles Logsdon, University of Washington). Based on an estimated width for Admiralty Inlet of ~7km and a vertical scale for the deep-water intrusion of ~50m (Fig. 2), we estimate the length of the intruding water mass should be about 20km in order to fill the bottom of the Main Basin as observed. Given that the distance between Sts. 1 and 7 is about 30km, the first hydrographic section has captured the bulk of the waters that penetrated below 170m into Puget Sound. Compared to past studies of intrusions (Cannon and Laird, 1978, Geyer and Cannon, 1982, Cannon et al., 1990) that were mostly observed using mooring data, this intrusion is one of the strongest. For average intrusions, changes in salinity are ~0.2psu (Geyer and Cannon, 1982), while being nearly 0.8psu here. While it was suggested (Lavelle et al., 1991) that the summer season should be the season of strongest intrusions, our measurements together with past studies (Op. Sit.) have shown the spring is a season of very strong intrusions. Reasons for the greater strength of spring intrusions are the maximum diurnal inequality, the relative weakness of the neap tides close to the equinox (Holbrook, personal communication), and the weakening of southerly winds that prevail during winter.

We find that biochemical tracers such as the concentration of oxygen, chl *a,* pheopigments and flow-cytometric analysis, although non-conservative, add to the standard Temperature-Salinity analysis in providing direct evidence for pathways of cells and cysts into the Main Basin of

Puget Sound. In addition these tracers provide a temporal signature and a constraints to biochemical processes, such as respiration. Since all have unique distributions in the sound and Admiralty Inlet, each provides slightly different information regarding the shape of the intrusion and its propagation.

The larger values of pheopigments associated with small particles could be indicative of high grazing rates by small zooplankton. Small dinoflagellates (Protoperidinium sp.) that feed on large diatom chains were observed in a water sample collected from the surface waters at St. 1 (S. Menden-Deuer, personal communication). Another possibility is that fecal pellets of larger zooplankton (~300μm copepods, B. Frost, personal communication) break within the water column or during filtration. Buck and Newton (1995) found in Debob Bay, Washington, that dinoflagellates were an important source of small fecal pellets. These pellets were devoid of pigments, although Strom (1993) has shown that the fecal pellets of certain dinoflagellates do contain pheopigments. Why pheopigments were more abundant in small particles, relative to chl *a*, in our samples remains an open question.

The loss of chl *a* between the two hydrographic sections could be due both to sinking of the large cells to the bottom and/or to conversion of chl *a* to pheopigments through zooplankton grazing with subsequent sinking of pellets. In both hydrographic sections the bulk of the measured pheopigments were from the fraction of particles smaller than 70μm. Small particles sink slower than large particles (assuming similar density), and thus are expected to stay longer in the water column.

A potential source of respired organic carbon in the Main Basin is Seattle's sewage outfall which can release up to 400 millions gallons of sewage a day with a maximum concentration of dissolved organic carbon of 30 mg/l. Assuming an extreme scenario, such that all the organic carbon gets oxidized within the deep water mass (i.e. an input of 1 part sewage for nearly 650

parts of deep water), the potential disappearance of only another 0.15ml l^{-1} oxygen can be explained. In order to achieve an oxygen mass balance we have to assume either that organic material is respired within the sediment (i.e. the sediments are a sink for the water column's oxygen) or that organic matter previously deposited on the bottom is resuspended by the intrusion and respired within the water column (indeed low transmittance is observed near the bottom). It is interesting to note that intrusions can both import relatively oxygenated surface waters as well as the biogenic material whose degradation will consume oxygen. The contribution of surface carbon to deep waters by sinking is a relatively unimportant route for carbon transport relative to advective transport by intrusion (Winter et al., 1975).

CONCLUSIONS

An intense intrusion of deep water into the Main Basin of Puget Sound was recorded. The intrusion is saltier (0.8psu) warmer (0.4°C) and denser (0.6Kg m^{-3}) than the water residing in the Main Basin prior to the intrusion (Fig. 4).

Fractionation of pigments data and the data derived using flow cytometry suggest that small cells are better preserved within the intrusion than large cells. The link between the size of particles containing pheopigments and the size of phytoplankton cell and their predators needs further study before it can be used as an indicator of trophic dynamics.

Two classes of small particles, with optical characteristics similar to cyanobacteria, were quantified. The particle with optical properties that resembled coastal cyanobacterial species dominated during our cruises. A third unidentified group of particles, which does not behave in a similar manner to the phytoplankton, was found in significant concentrations near the bottom of Puget Sound. The most abundant group (F1) was shown to be a useful tracer for downwelling waters (Fig. 6). Under dark conditions, it had a half-life time of about 6 days, a period long

enough to be observed through the intrusion penetration and short enough to decrease prior to the entry of a new intrusion.

Winter et al. (1975) have studied the dynamics of pigments during spring and summer in Puget Sound. They found large concentration of pigments (they did not separate chl *a* and pheopigments) to occur at a fortnightly periodicity, in association with increased salinity in the bottom. They have hypothesized that bottom water renewal processes are the underlying mechanism, a hypothesis we were able to confirm. Here we find that more than 80% of the chl *a* concentration disappeared from the bottom waters within a week time, an indication of the rapid consumption and/or sinking of the pigments in the deep-water intrusion. The impact on oxygen was rapid with a reduction of ~0.6ml l^{-1} in one week. Whether the reduction is solely due to the intrusion still needs to be determined.

The predictability of major circulation features in Puget Sound, as highlighted here for a deep-water intrusion, could be used to maximize the rate of transport of anthropogenic contaminants away from Puget Sound into the Strait of Juan de Fuca. On average, 52% of the water entering Admiralty Inlet from Puget Sound recirculates into other Puget Sound layers (Cokelet et al., 1991). But timing the release of contaminants and adjusting their density so that the smallest amount gets refluxed into the Sound at the sill, should lower the refluxing ratio of contaminants significantly. Use of numerical models that assimilate hydrographic and wind data at key locations in Puget Sound would increase greatly the ability to accurately predict the circulation in Puget Sound.

ACKNOWLEDGMENT

We would like to thank the Washington Sea Grant Program for supporting this project. The University of Washington Royalty Research Fund provided additional funds. Al Mojfeld provided tidal data; G. Cannon and J. Holbrook provided information about past intrusions. Lee Karp-Boss provided an excellent review of an earlier draft of this paper. The data could not have been collected without the help of the technical staff and of graduate students of the School of Oceanography at the University of Washington.

REFERENCES

Bretschneider, D. E., G. A. Cannon, J. R. Holbrook, and D. J. Pashinski, 1985. Variability of subtidal current structure in a fjord estuary: Puget Sound, Washington, Journal of Geophysical Research, 90: 11949-11958.

Buck, K. R., and J. Newton, , 1995. Fecal pellet flux in Dabob Bay during a diatom bloom: contribution of microzooplankton, Limnology and Oceanography, 40: 36-315.

Cannon, G. A., and N. P. Laird, 1978. Variability of currents and water properties from year-long observation in a fjord estuary, p. 515-535, In J. D. Nihoul (ed.), Hydrodynamics of estuaries and fjords, Elsevier, Amsterdam.

Cannon, G. A., J. R. Holbrook, and D. J. Pashinski, 1990. Variations in the onset of bottom-water intrusions over the entrance sill of a fjord, Estuaries, 13: 31-42.

Cokelet, E. D., R. J. Stewart and C. C. Ebbesmeyer, 1991. Concentrations and ages of conservative pollutants in Puget Sound, Proceedings, Puget Sound Research '91, 1: 99-108, Puget Sound Water Quality Authority, Seattle.

Ebbesmeyer, C. C. and C. A. Barnes, 1980. Control of a fjord basin's dynamics by tidal mixing in embracing sill zones, Estuarine and Coastal Marine Science, 11: 311-330.

Farmer, D. M. and H. J. Freeland, 1983. The physical oceanography of fjords, Progress in Oceanography, 12: 147-220.

Geyer, W. R., and G. A. Cannon, 1982. Sill processes related to deep-water renewal in a fjord. Journal of Geophysical Research, 87: 7985-7996.

Holm-Hansen, O., C. J. Lorenzen, R. W. Holmes, and J. D. H. Strickland, 1965. Fluorometric determination of chlorophyll, Journal du Conseil Permanent International Pour L'Exploration de la Mer , 30: 3-15.

Lavelle, J. W., E. D. Cokelet and G. A. Cannon, 1991. A model study of density intrusions into and circulation within a deep, silled estuary: Puget Sound, Journal of Geophysical Research, 96: 16779-16800.

Olson, R. J., S. W. Chilsholm, E. R. Zettler and E. V. Armbrust, 1988. Analysis of *Synechococcus* pigment types in the sea using single and dual beam flow cytometry, Deep Sea Researcg, 35: 425-440.

Roemmich, D., 1983.Optimal estimation of hydrographic station data and derived fields, Journal of Physical Oceanography, 13: 1544-1549.

Strom, S. L., 1993. Production of phaeopigments by marine protozoa: results of laboratory experiments analyzed by HPLC., Deep Sea Research, 40: 57-80, 1993.

Turner, J. A., and M. C. Gregg, 1995. High resolution observations of sill dynamics in Puget Sound, *Proceedings, Puget Sound Research '95*, 2: 789-803, Puget Sound Water Quality Authority, Olympia, 1995.

Winter, D. F., K. Banse and G. C. Anderson, 1975. The dynamics of phytoplankton blooms in Puget Sound, a fjord in the northwestern United States, Marine Biology, 29: 139-176.

	σ_θ [Kg m^{-3}]	θ [°C]	O_2 [ml l^{-1}]	chl *a* [mg m^{-3}]	Chl_*a* >70μm	Pheo [mg m^{-3}]	Pheo >70μm
Section- I	23 (0.1)	8.45 (0.01)	8.6 (0.3)	2.3 (0.4)	0.9 (0.2)	0.9 (0.3)	0.16 (0.1)
Section- II	23 (0.1)	8.32 (0.01)	8 (0.1)	0.4 (0.1)	0.1 (0.05)	0.9 (0.4)	0.02 (0.02)
10a(202m)	22.6	8	7.98	0.24(.02)	0.03	0.42(.05)	0.07

Table 1: Average water properties within the deep-water intrusion (23.2 > σ_θ > 22.9), and standard deviations (in parenthesis), based on interpolation by objective analysis (see Fig. 2 for symbols and units). St. 10a water properties at 202m, measured prior to the intrusion, are given for reference.

Figure captions:

Figure 1. Map of Puget Sound, WA, with location of stations and Seattle tides during the period of the study . Stations 1 to 10 were occupied during the intrusions on 13-14 April 1997 (section C-I); stations 10 to 18 were occupied one week after the intrusion on 20 April 1997 (C-II). Station 201 was occupied on April 17 1997.

Figure 2. Density (σ_θ), potential temperature (θ), oxygen (O_2), total chl *a* (chlorophyll *a*), frac chl *a* (chl *a* associated with particles > 70m), total pheopigment (pheo), and frac pheo (pheo associated with particles > 70m) during the two sections. Insets in top panels depict the tidal heights when each transect took place. Contour values drawn in panels of each property are provided in the right panel of each property.. Bold lines represent the isopycnal that defines the deep water intrusion (σ_θ=23-23.5). Dots denote position where samples were taken.

Figure 3. Flow cytometeric analysis of bottom water from St. 16. Three classes of particles are distinguished based on chlorophyll a fluorescence (Red F.), phycoerythrin fluorescence (Orange F.) and forward scatter, an indication of particle size. The F1 particles are uniquely distinguished by their lower orange fluorescence, while the F2 and F3 particles are distinguished based on differences in forward scatter. The distributions of F1 and F2 within the water column is given in Fig. 6.

Figure 4. Potential temperature (θ) -salinity diagram of representative stations from both hydrographic sections with over-layed density (σ_θ) contours. The source of the bottom waters (σ_θ>23) can be traced to St. 1. The water that was resident in the Main Basin prior to the

intrusion (bottom of St. 10a) was lifted higher into the water column by the intrusion (St. 10c). The influence of Whidbey Basin waters (St. 201) can be observed closer to the surface (e.g. St. 10b for $\sigma_\theta \approx 22.25$).

Figure 5. Density (σ_θ), salinity, potential temperature (θ), percent (%) light transmittance at St. 10 before (St. 10a) and after bottom intrusions entered Puget Sound (St. 10 b, c, and d).

Figure 6. Distribution of two groups of particles classified from flow cytometric analysis (see Fig. 3), F1 (similar in fluorescence and scattering patterns as S. bacillaris, clone SYNG, top panel), and F2 (similar in fluorescence and scattering patterns as *Synechococcus* WH7803, clone SYNDC2, middle panel), respectively a coastal and a pelagic cyanobacterium (Olson et al., 1988) in cell number per 200µl. Bottom panel denotes the ratio, F2/F1.

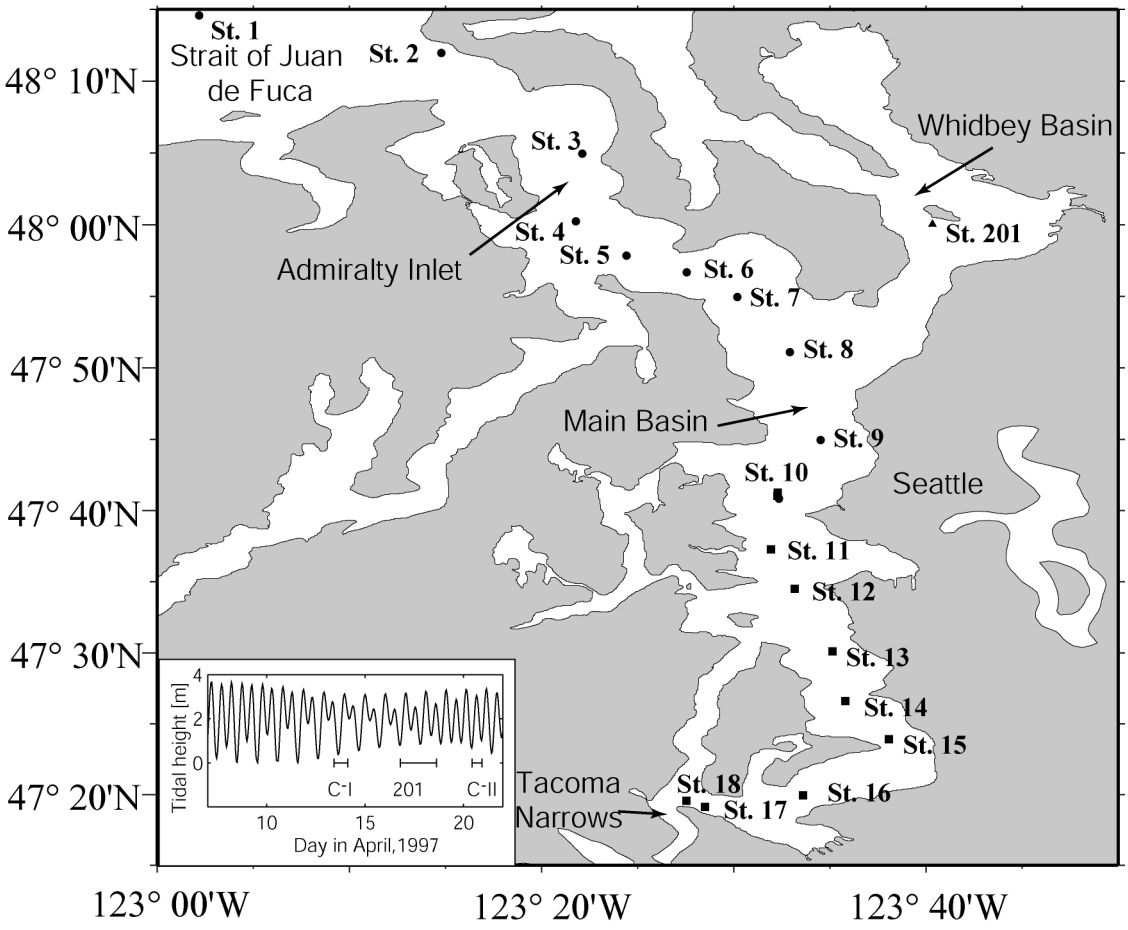
St. 1
Strait of Juan de Fuca
St. 2
St. 3
St. 4
St. 5
St. 6
St. 7
St. 8
St. 9
St. 10
St. 11
St. 12
St. 13
St. 14
St. 15
St. 16
St. 17
St. 18
St. 201
Whidbey Basin
Admiralty Inlet
Main Basin
Seattle
Tacoma Narrows
48° 10'N
48° 00'N
47° 50'N
47° 40'N
47° 30'N
47° 20'N
123° 00'W
123° 20'W
123° 40'W
Tidal height [m]
C-I
201
C-II
Day in April,1997

Figure 1

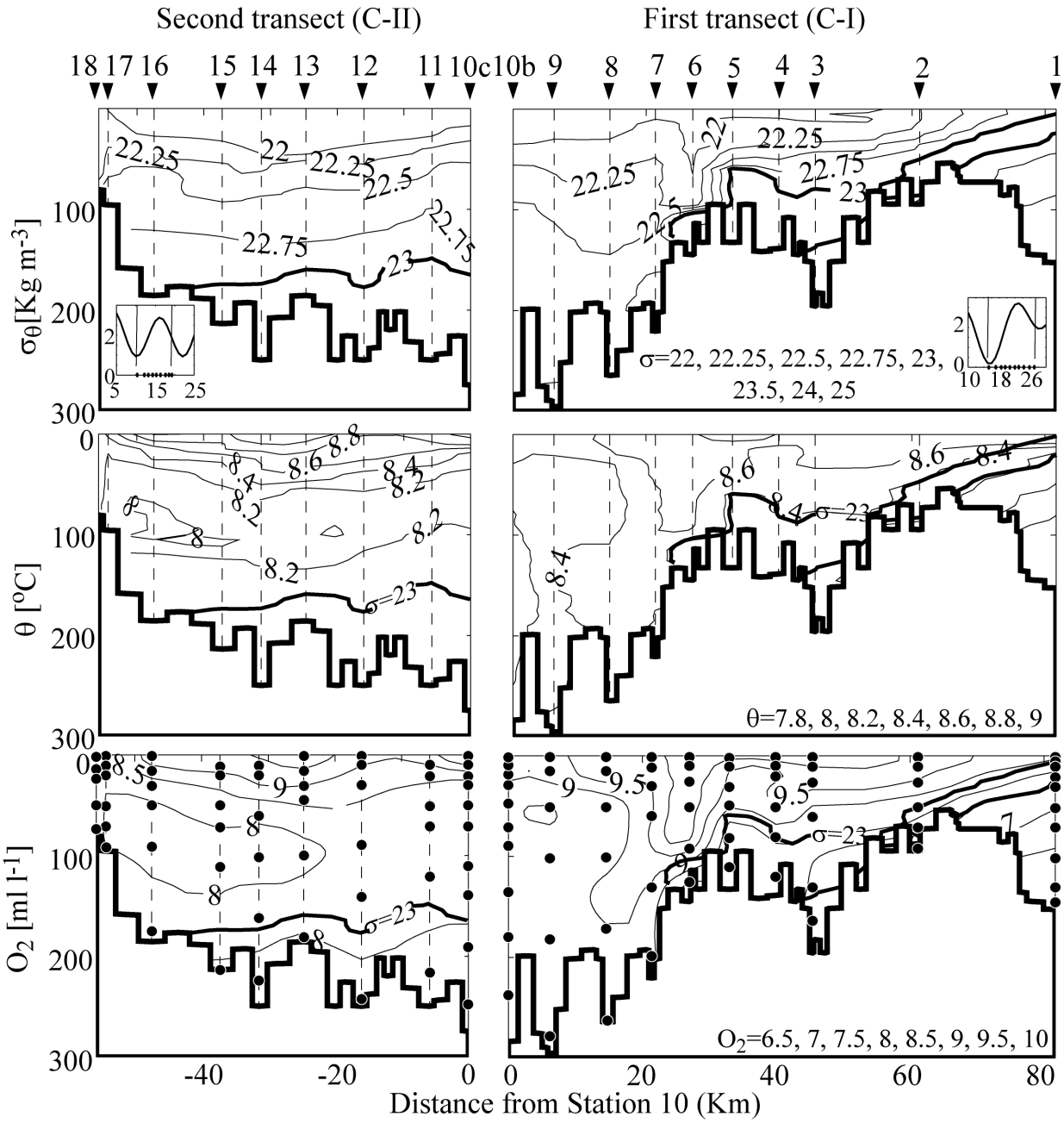
Second transect (C-II)
First transect (C-I)
18 17 16 15 14 13 12 11 10c 10b 9 8 7 6 5 4 3 2 1
σθ[Kg m-3]
θ [°C]
O2 [ml l-1]
σ=22, 22.25, 22.5, 22.75, 23, 23.5, 24, 25
θ=7.8, 8, 8.2, 8.4, 8.6, 8.8, 9
O2=6.5, 7, 7.5, 8, 8.5, 9, 9.5, 10
Distance from Station 10 (Km)

Figure 2a

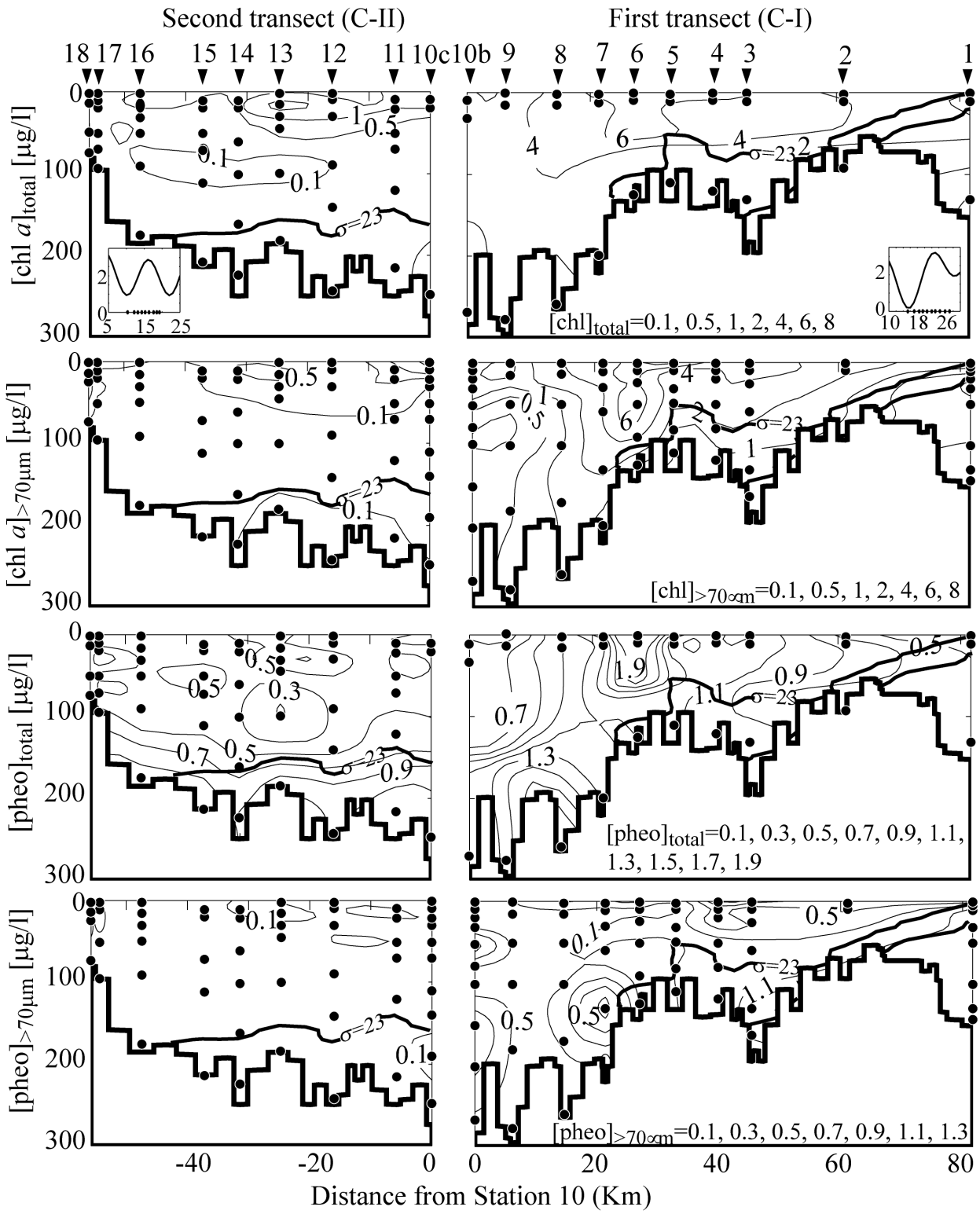
Second transect (C-II)
First transect (C-I)
18 17 16 15 14 13 12 11 10c 10b 9 8 7 6 5 4 3 2 1
[chl a]total [µg/l]
[chl a]>70µm [µg/l]
[pheo]total [µg/l]
[pheo]>70µm [µg/l]
σ=23
[chl]total=0.1, 0.5, 1, 2, 4, 6, 8
[chl]>70∝m=0.1, 0.5, 1, 2, 4, 6, 8
[pheo]total=0.1, 0.3, 0.5, 0.7, 0.9, 1.1, 1.3, 1.5, 1.7, 1.9
[pheo]>70∝m=0.1, 0.3, 0.5, 0.7, 0.9, 1.1, 1.3
Distance from Station 10 (Km)

Figure 2b

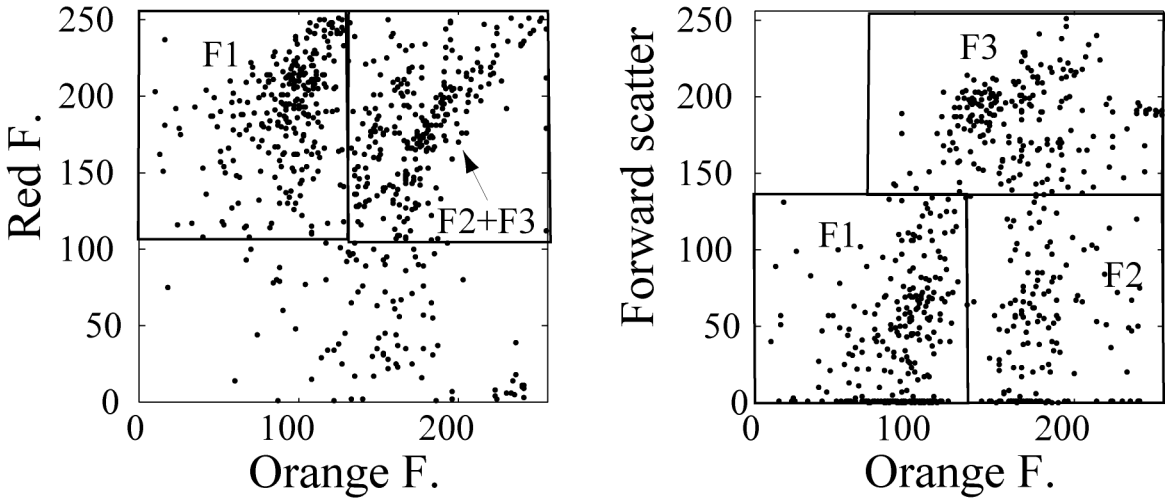
Red F.
Orange F.
F1
F2+F3
Forward scatter
Orange F.
F3
F1
F2
0
50
100
150
200
250

Figure 3

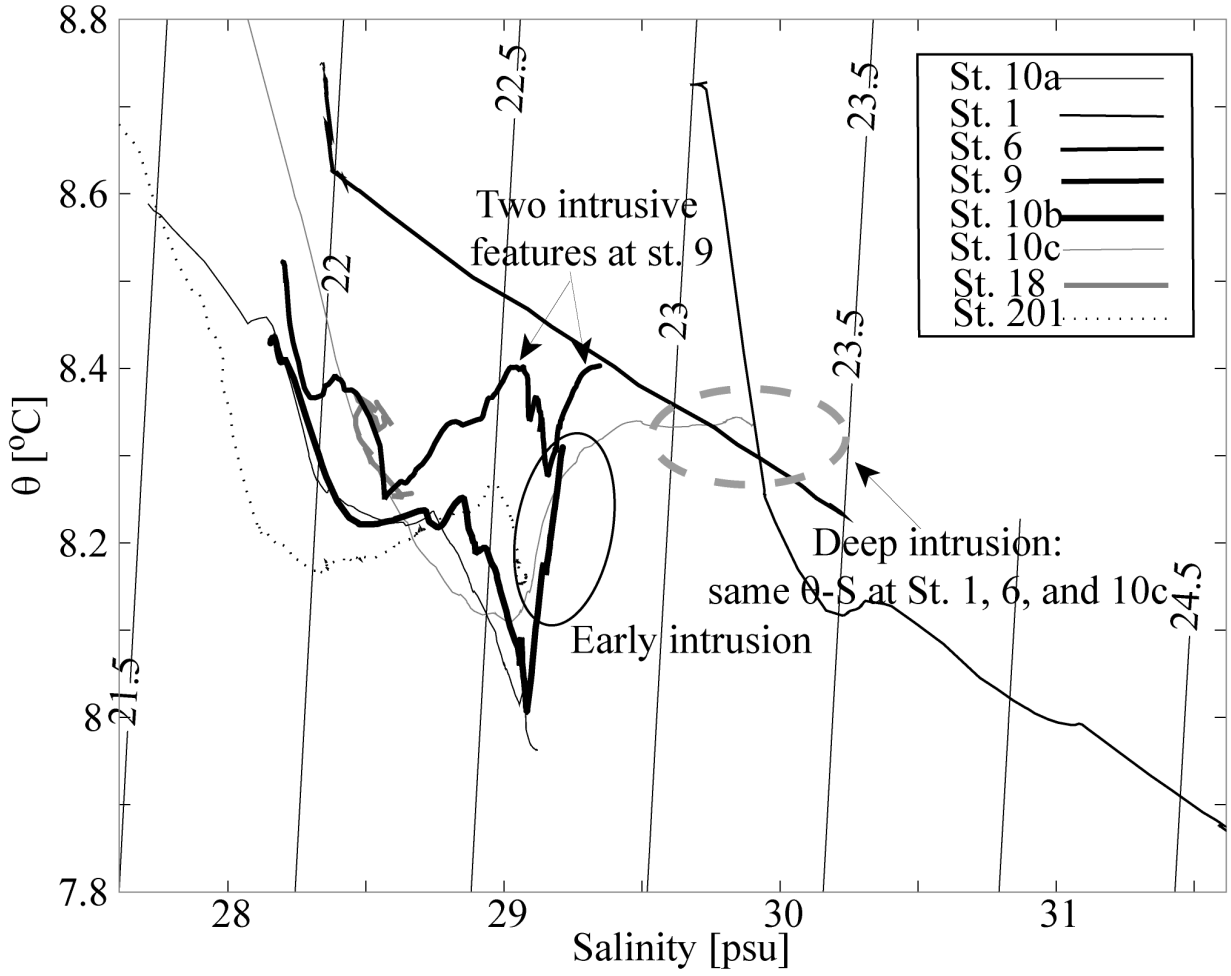
8.8
8.6
8.4
8.2
8
7.8
θ [°C]
28
29
30
31
Salinity [psu]
21.5
22
22.5
23
23.5
23.5
24.5
St. 10a
St. 1
St. 6
St. 9
St. 10b
St. 10c
St. 18
St. 201
Two intrusive features at st. 9
Early intrusion
Deep intrusion: same θ-S at St. 1, 6, and 10c

Figure 4

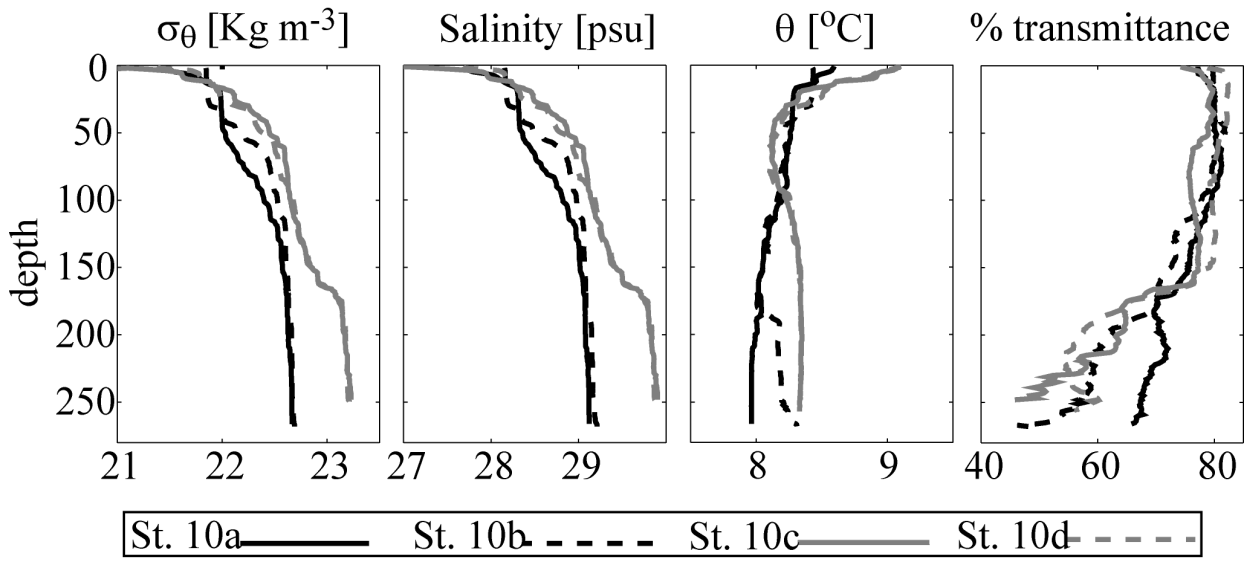
σθ [Kg m-3]
Salinity [psu]
θ [oC]
% transmittance
depth
0
50
100
150
200
250
21
22
23
27
28
29
8
9
40
60
80
St. 10a
St. 10b
St. 10c
St. 10d

Figure 5

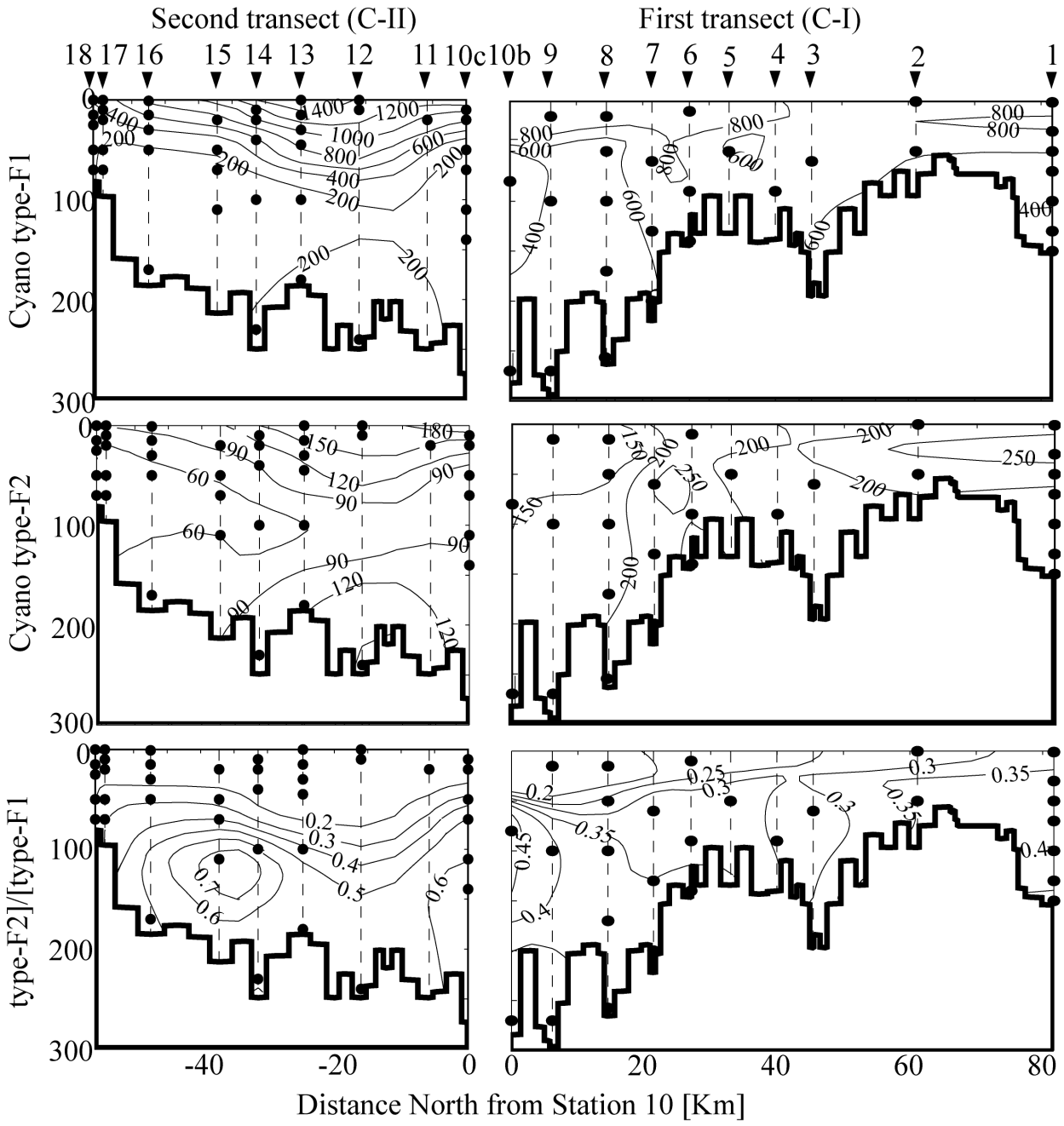
Second transect (C-II)
First transect (C-I)
18 17 16 15 14 13 12 11 10c 10b 9 8 7 6 5 4 3 2 1
Cyano type-F1
Cyano type-F2
type-F2]/[type-F1
Distance North from Station 10 [Km]

Figure 6